## EDGE ARTICLE

ROYAL SOCIETY OF CHEMISTRY

# Synthesis, bridgehead functionalization, and photoisomerization of 9,10-diboratatriptycene dianions†

Sven E. Prey,[a] Jannik Gilmer,[a] Samira V. Teichmann,[a] Luis Čaić,[a] Mischa Wenisch,[a] Michael Bolte,[a] Alexander Virovets,[a] Hans-Wolfram Lerner,[a] Felipe Fantuzzi[b] and Matthias Wagner *[a]

9,10-Diboratatriptycene salts $M_2[RB(\mu\text{-}C_6H_4)_3BR]$ (R = H, Me; $M^+$ = $Li^+$, $K^+$, $[n\text{-}Bu_4N]^+$) have been synthesized *via* [4 + 2] cycloaddition between doubly reduced 9,10-dihydro-9,10-diboraanthracenes $M_2[DBA]$ and benzyne, generated *in situ* from $C_6H_5F$ and $C_6H_5Li$ or $LiN(i\text{-}Pr)_2$. $[HB(\mu\text{-}C_6H_4)_3BH]^{2-}$ reacts with $CH_2Cl_2$ to form quantitatively the bridgehead-derivatized $[ClB(\mu\text{-}C_6H_4)_3BCl]^{2-}$, while twofold $H^-$ abstraction with $B(C_6F_5)_3$ in the presence of $SMe_2$ leads cleanly to the diadduct $(Me_2S)B(\mu\text{-}C_6H_4)_3B(SMe_2)$. Photoisomerization of $K_2[HB(\mu\text{-}C_6H_4)_3BH]$ (THF, medium-pressure Hg lamp) provides facile access to diborabenzo[a]fluoranthenes, a little explored form of boron-doped polycyclic aromatic hydrocarbons. According to DFT calculations, the underlying reaction mechanism consists of three main steps: (i) photoinduced di-π-borate rearrangement, (ii) "walk reaction" of a BH unit, and (iii) boryl anion-like C–H activation.

## Introduction

The terms "aromatic hydrocarbon" and "planar π system" can be used as synonyms for most representatives of these substance classes. Triptycenes are among the few aromatic hydrocarbons that enter the third dimension, which is one reason why they have fascinated the chemical community for decades. Triptycene is built upon a [2.2.2]-bicyclic system with three 1,2-phenylene blades to generate a $D_{3h}$-symmetric paddle-wheel scaffold.[1,2] Due to its exceptional rigidity, the triptycene framework has been used as a backbone for transition-metal ligands[3,4] and as a building block for molecular motors.[5] When incorporated into emitting polymers, triptycene units can sterically block the individual polymer chains so that the materials exhibit solution-like luminescence properties in the solid state, with applications in sensor technology.[6] The three-dimensional shape of a triptycene building block creates a free volume around the molecule (*i.e.*, between the blades of the paddle-wheel structure), which can be designed such that it confers size selectivity in sensory responses,[7] promotes the

desired alignment in oriented polymers,[8] or creates porous organic materials.[9] Of more academic interest – but no less fascinating – is the excited-state reactivity of triptycene and the resulting photorearrangement products (*i.e.*, a norcaradiene and a benzo[a]fluoranthene derivative).[10,11]

A proper means of expanding the chemical space of triptycenes as well as their application potential is heteroatom doping, *i.e.*, the replacement of selected C atoms by other p-block elements. Our group has a long-standing interest in triptycenes featuring B atoms at their bridgehead positions. One example is the $(BN)_2$-triptycene **A** (Fig. 1). **A**-type structures are accessible by simple mixing of 9,10-dihydro-9,10-diboraanthracenes (DBAs) with 1,2-diazenes, such as pyridazine. Since the reaction is based on the essentially barrierless formation of a double B–N adduct, **A** is obtained in very good yields of ≈80%.[12–14] An organometallic $(BN_2)_2$-triptycene is the pyrazabole-bridged *ansa*-ferrocene **B** (Fig. 1).[15] Recently, our group succeeded in abstracting one of its bridgehead $H^-$ ligands and characterized the resulting free, cationic Lewis superacid $[\mathbf{B} - H]^+$ by X-ray crystallography.[16] Berionni and coworkers reported a series of boratatriptycenes **C** (Fig. 1) possessing various different atoms/groups "E" at the second bridgehead position (E = CH, $PH^+$, $S^+$, $Se^+$).[17–20] A derivative of **C** combining E = CH and Ar = 4-*t*-Bu-$C_6H_4$ underwent selective protodeboronation of the exocyclic C–B bond upon treatment with bistriflimidic acid ($HNTf_2$); the resulting boratriptycene Lewis acid still engages in a dynamic association–dissociation equilibrium with the weakly coordinating $[NTf_2]^-$ anion.[18] This finding underscores the potential for enhancing Lewis acidity

[a]*Institut für Anorganische und Analytische Chemie, Goethe-Universität Frankfurt, Max-von-Laue-Straße 7, D-60438 Frankfurt am Main, Germany. E-mail: matthias.wagner@chemie.uni-frankfurt.de*

[b]*School of Chemistry and Forensic Science, University of Kent, Park Wood Rd, Canterbury CT2 7NH, UK*

† Electronic supplementary information (ESI) available: Synthetic procedures, NMR spectra, X-ray crystallographic data and computational details. CCDC 2238019–2238023. For ESI and crystallographic data in CIF or other electronic format see DOI: https://doi.org/10.1039/d3sc00555k
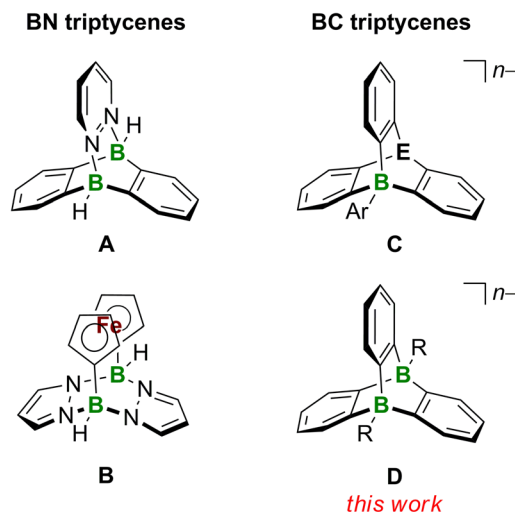
**BN triptycenes**          **BC triptycenes**



Fig. 1 Boron-containing triptycenes. Left: the DBA-pyridazine adduct **A** and the 1,1'-ferrocenediyl-bridged pyrazabole **B** as BN derivatives of triptycene. Right: Berionni's BC-triptycenes **C** featuring one B atom at a bridgehead position (E = CH, $n = 1$; E = PH$^+$, S$^+$, Se$^+$, $n = 0$; Ar = aryl) and the dibora(ta)triptycenes **D** presented in this work (R = H, Me, $n = 2$; R = SMe$_2$, $n = 0$). DBA = 9,10-dihydro-9,10-diboraanthracene.



Scheme 1 Synthesis of 9,10-diboratatriptycenes by either sequential B–C-adduct formation (left) or [4 + 2] cycloaddition of in situ-generated benzynes with M$_2$[DBA] salts (right). (i) 1,2-C$_6$H$_4$I$_2$, t-BuLi, THF/Et$_2$O (1 : 1), −110 °C → room temperature, overnight, 21% yield; (ii) 1,2-C$_2$H$_4$Br$_2$ (6 mol%), THF, room temperature, 3 d; (iii) THF, room temperature, 1 h, quant. conv. by NMR; (iv) C$_6$H$_5$F (1–2 equiv.), base (LiN(i-Pr)$_2$ or C$_6$H$_5$Li), THF, −78 °C → room temperature, overnight to 5 d, Li$_2$[5]: 50–75% yield, K$_2$[6]: 41% yield, K$_2$[7]: few crystals.
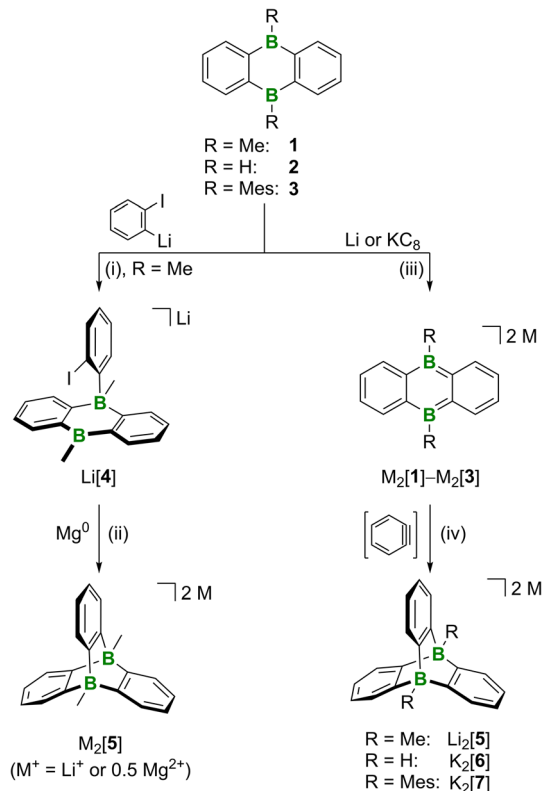
by designing a rigid organic framework in a way to impose a structural constraint on the BC$_3$ core that forces it out of planarity (see also the Lewis superacidity of $[\text{B} - \text{H}]^+$ mentioned above[16]).[17]

From the application examples of triptycenes, it is obvious that the degree of repulsive or attractive interactions between the paddle-wheels' blades and their immediate environments play an important role. Since these interactions will be strongly influenced by the overall charge of the triptycene scaffold, we are herein targeting dianionic diboratatriptycenes **D** (Fig. 1; R = H, Me; $n = 2$). We will show that H$^-$ abstraction in situ releases a Lewis acid with potentially cooperating B atoms[21] and allows convenient derivatization of both bridgehead positions. We finally show that the photorearrangement of **D** (R = H; $n = 2$) provides access to the little explored compound class of diborabenzo[a]fluoranthenes.[22]

## Results and discussion

### Synthesis of 9,10-diboratatriptycenes D

We tested two conceptually different ways to prepare our **D**-type target compounds: (a) adduct formation on neutral DBA and (b) [4 + 2] cycloaddition on doubly reduced [DBA]$^{2-}$. The first approach (a) is inspired by the facile synthesis of **A** and based on the assumption that pyridazine can, in principle, be replaced by the isoelectronic benzene-1,2-diide to assemble the tricyclic scaffold of **D** via a twofold B–C-adduct formation. Unfortunately, the available literature on 1,2-dimetalated benzenes indicates a rather limited synthetic value of these highly reactive species.[23] We therefore resorted to a stepwise reaction protocol, starting from in situ-prepared o-iodophenyllithium and **1** (−110 °C, THF/Et$_2$O (1 : 1); Scheme 1).[24] Cyclization of the obtained B(sp$^2$)–B(sp$^3$) intermediate Li[**4**] was subsequently

accomplished by stirring with Mg$^0$ (room temperature, THF). Since the NMR-spectroscopic investigation of the crude product still showed the formation of some unwanted side products that later proved difficult to remove, the B–C-adduct approach was eventually abandoned in favor of the Umpolung strategy (b): given that doubly reduced DBAs easily undergo [4 + 2]-cycloaddition reactions with (hetero)olefins or internal alkynes,[25] the reaction of DBA salts M$_2$[**1**]–M$_2$[**3**] with in situ-generated benzyne should likewise generate diboratatriptycenes M$_2$[**5**]–M$_2$[**7**] (Scheme 1). For an initial proof-of-principle experiment, we selected Li$_2$[**1**], because we have had good experience with cycloadditions on this compound in the past.[25] LiN(i-Pr)$_2$ in THF was added with stirring at −78 °C to a mixture of freshly prepared Li$_2$[**1**] (ref. 26 and 27) and C$_6$H$_5$F in THF (Scheme 1). After warming to room temperature overnight, the reaction mixture had lost the characteristic red color of Li$_2$[**1**] and turned to pale yellow. $^{11}$B NMR spectroscopy showed the selective formation of one new species; its chemical shift value of $\delta(^{11}\text{B}) = -13.2$ ppm testified to the presence of tetra-coordinated B atoms.[28] An $^1$H NMR spectrum, recorded on the crude product after a solvent change to THF-$d_8$, indicated an essentially quantitative conversion: a signal at 0.56 ppm (6H)

and two resonances at 7.24 (br, 6H) and 6.44 ppm (m, 6H) are assignable to two chemically equivalent $CH_3$ groups and three chemically equivalent $C_6H_4$ rings, respectively. Also the $^{13}C\{^1H\}$ NMR spectra supported the proposed $D_{3h}$-symmetric molecular structure of $[5]^{2-}$ in solution. Purification of $Li_2[5]$ through crystallization from THF gave yields of 50–75% (attempts at X-ray analysis were not successful). Next, we moved on from DBA **1** to DBA **2** to also get a hold of the parent diborata-triptycene. $K_2[6]$ was prepared in a similar manner as $Li_2[5]$ and isolated in 41% yield ($\delta(^{11}B) = -8.3$ ppm, d, $^1J(B,H) = 87$ Hz); the BH resonance was found at 3.36 ppm in the $^1H\{^{11}B\}$ NMR spectrum.[29] To stress the steric limits of the [4 + 2] cycloaddition, we finally treated dimesitylated $K_2[3]$ with benzyne and still obtained $K_2[7]$, albeit in negligible yield of only a few crystals.[24]

Crystals of $[K(dme)][K(dme)_2][6]$ suitable for X-ray diffraction (XRD) were obtained from a gas-phase diffusion experiment (*n*-hexane/1,2-dimethoxyethane (DME); Fig. 2). In $[K(dme)]$-$[K(dme)_2][6]$, the diboratatriptycene dianion $[6]^{2-}$ acts as chelating ligand toward both $K^+$ ions (*via* the π-electron clouds of its 1,2-phenylene rings). The coordination sphere of $K(1)^+$ is completed by two dme ligands; $K(2)^+$ carries only one dme ligand and is further bonded to two phenylene rings of an adjacent $[6]^{2-}$ moiety, thereby creating a coordination polymer in which all three pockets of the paddle-wheel anion are occupied by $K^+$ ions (Fig. S61†). The six B–C-bond lengths of $C_1$-symmetric (in the crystal lattice) $[6]^{2-}$ range from 1.620(3) to 1.643(3) Å (avg. 1.631 Å) and are comparable to those in the structurally unconstrained, acyclic analogue $[HBPh_3]^-$ (1.628(6) to 1.633(6) Å, avg. 1.631 Å).[30] Of the three dihedral angles 107.9°, 124.8°, and 127.3° between phenylene rings, the smallest is associated with the pocket hosting the doubly $\eta^6$-coordinated $K(1)^+$.

### Activation of the B–H bonds of the 9,10-diboratatriptycene $[6]^{2-}$

Having the diboratatriptycene salt $[K(dme)][K(dme)_2][6]$ in hand, we next addressed the question of how to activate its B–H bonds to derivatize the bridgehead positions and/or generate the free Lewis acid *in situ*. The neutral ditopic Lewis acid **S1** (Scheme 2) should be among the strongest neutral B-based
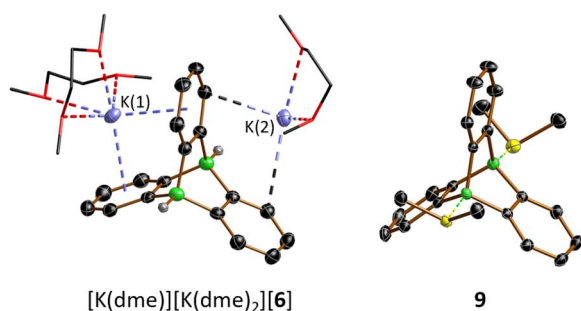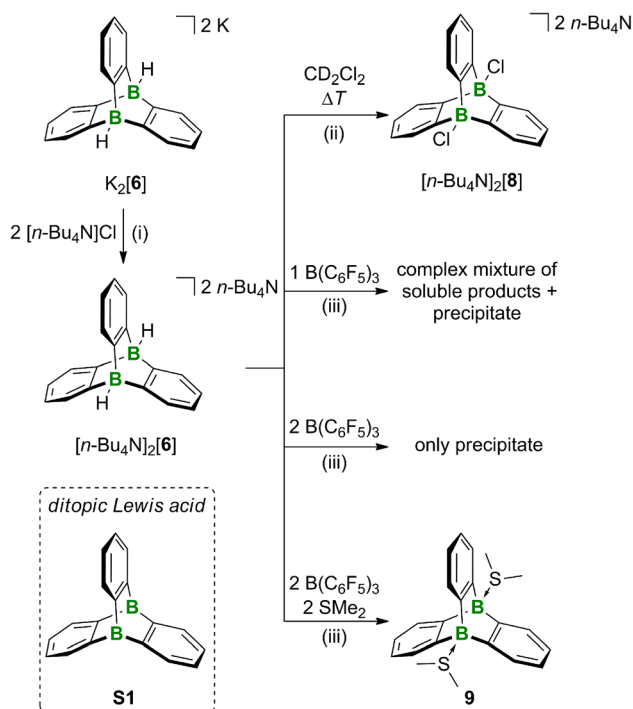


Fig. 2 Solid-state structures of $[K(dme)][K(dme)_2][6]$ and **9** with thermal ellipsoids shown at the 50% probability level; C-bonded H atoms and a non-coordinating $CH_2Cl_2$ molecule in the crystal lattice of **9** are omitted for clarity, dme ligands are depicted as wireframes. H: gray, B: green, C: black, O: red, S: yellow, K: light blue.



Scheme 2 Reactivity of 9,10-diboratatriptycene $[6]^{2-}$. (i) (1) THF, room temperature, 1 h; (2) extraction into $CH_2Cl_2$, 93% yield; (ii) 50 °C, 18 h, 89% yield; (iii) $CD_2Cl_2$, room temperature, 5 min, **9**: quant. conv. by NMR.

acids, as judged by its computed $F^-$-ion affinity $FIA_{solv}(\text{**S1**})$ of 384 kJ mol$^{-1}$ (*cf.* $FIA_{solv}(B(C_6F_5)_3) = 315$ kJ mol$^{-1}$; solv = $CH_2Cl_2$; for FIAs of further $B_2$-triptycenes and a more detailed discussion see the ESI†).[16] As the dme ligands present in the complex cations could potentially become B-coordinating and thereby interfere with the planned reactivity studies, we first performed a cation exchange with $[n\text{-}Bu_4N]Cl$ in THF. $[n\text{-}Bu_4N]_2[6]$ precipitates together with KCl from the reaction mixture and was separated from the latter by extraction into $CH_2Cl_2$ (93% yield). Care must be taken to remove the solvent from the product in time after workup to avoid B–H/B–Cl exchange.[31] On the other hand, the reaction between $[n\text{-}Bu_4N]_2[6]$ and $CH_2Cl_2$ can be used for the straightforward synthesis of bridgehead-chlorinated $[n\text{-}Bu_4N]_2[8]$ (14 d at room temperature or 18 h at 50 °C; 89% yield; Scheme 2). In an attempt to release the free monotopic Lewis acid, $[n\text{-}Bu_4N]_2[6]$ was treated with 1 equiv. of $B(C_6F_5)_3$ in $CD_2Cl_2$. NMR spectroscopy showed that $B(C_6F_5)_3$ had been quantitatively transformed to $[n\text{-}Bu_4N][HB(C_6F_5)_3]$, even though some unconsumed starting material $[n\text{-}Bu_4N]_2[6]$ remained in the mixture. Several non-identified species and small quantities of a precipitate had formed. When the amount of $B(C_6F_5)_3$ added was increased to 2 equiv., the $H^-$ scavenger was still fully converted, phenylene resonances were no longer detectable in the $^1H$ NMR spectrum, and substantial amounts of precipitate were found in the NMR tube. A similar result was obtained when $[Ph_3C][B(C_6F_5)_4]$ was used instead of $B(C_6F_5)_3$. The precipitate could not be re-dissolved by addition of $SMe_2$. The situation changed when the double $H^-$ abstraction was carried

out with $B(C_6F_5)_3$ in the presence of $SMe_2$, which led to the clean formation of the diboratriptycene–$SMe_2$ diadduct **9** (Scheme 2). Based on the computed FIAs of relevant $B_2$-triptycenes, we propose that the formation of **9** proceeds in a stepwise manner without intermediate formation of **S1**.[24] X-ray quality crystals of **9**·$CH_2Cl_2$ were grown from $CH_2Cl_2$ (Fig. 2).

The ^{11}B NMR spectrum of **9** is characterized by a signal at −1.4 ppm, in the region of tetracoordinated B nuclei.[28] The ^{1}H/^{13}C resonances of the $SMe_2$ ligands appear at 3.07/21.1 ppm ($CD_2Cl_2$), significantly downfield-shifted from those of free $SMe_2$ (2.09/18.4 ppm) and even $Me_2S$–$B(C_6F_5)_3$ (2.17/20.8 ppm;[32] $CDCl_3$), thus indicating a strong S–B-adduct bond. This conclusion is further confirmed by the short S–B-bond lengths of **9** (1.9710(19), 1.9775(18) Å; *cf.* $Me_2S$–$B(C_6F_5)_3$: S–B = 2.091(5) Å (ref. 33)).

To summarize, we assume that after $H^-$ abstraction on $[6]^{2-}$, the corresponding free Lewis acid **S1** is not stable but rather forms the insoluble solid by rearrangement or ring-opening polymerization. Although the structure of the solid remains to be confirmed, a plausible candidate is a polymer composed of 1,2-phenylene-bridged DBAs (Fig. S15†). The formation of a precipitate is suppressed if $SMe_2$ is present from the beginning to stabilize the diboratriptycene.

## Photoisomerization of the 9,10-diboratatriptycene $[6]^{2-}$

In contrast to the thermal rearrangement of free neutral diboratriptycene, photoisomerization of the diboratatriptycene salt $K_2[6]$ results in the well-defined, soluble product $K_2[10]$ (Scheme 3). $K_2[10]$ can be viewed as a molecule in which a DBA moiety shares one B atom and one phenylene ring with a $9H$-9-borafluorene unit.

Irradiation of a THF solution of $K_2[6]$ with a medium-pressure Hg lamp in a quartz vessel for 1 h led to a color change from colorless to yellow.[34] NMR spectroscopy on a THF-$d_8$ solution revealed the highly selective formation of $K_2[10]$. Its ^{11}B NMR spectrum shows a doublet ($\delta(^{11}B) = -13.7$ ppm, $^1J(B,H) = 73$ Hz) and a pseudo-triplet ($\delta(^{11}B) = -16.7$ ppm, $^1J(B,H) = 78$ Hz), assignable to a BH- and a $BH_2$ group, respectively. The corresponding $BH_n$ resonances were found in the $^1H\{^{11}B\}$ NMR spectrum at 2.65 (BH) and 2.52/2.40 ppm ($BH_2$). The $^{13}C\{^1H\}$ NMR spectrum supports the proposed $C_1$-symmetric molecular structure, since we observe 18 signals belonging to three different six-membered rings (according to $^1H$-$^{13}C$-HSQC and -HMBC experiments). Of those signals, five are severely broadened due to $^1J(B,C)$ coupling and the

quadrupolar effect of the $^{10/11}B$ nuclei and therefore correspond to the five required B-bonded C atoms; deshielded, quaternary $^{13}C$ atoms giving rise to NMR resonances at 151.1/144.3 ppm point toward the presence of a biphenyl fragment in the molecule. Moreover, the DFT-computed $^{13}C$ shift values of $[10]^{2-}$ agree well with the experimentally observed ones for $K_2[10]$ (avg. deviation: 2.0 ppm).[24] In order to gain more information on the mechanism underlying the photoisomerization of $[6]^{2-}$ to $[10]^{2-}$, we performed corresponding quantum-chemical calculations.

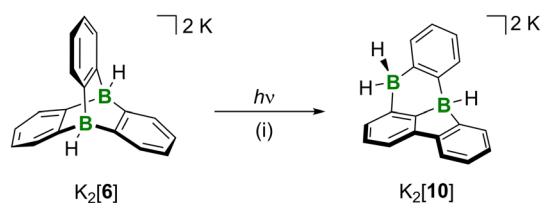## Assessment of the photoisomerization of $K_2[6]$ by theory

All energies were calculated at the SMD(THF)[35]/$\omega$B97XD[36]/6-311++G** level of theory, with optimized structures at SMD(THF)/$\omega$B97XD/6-31+G**. Vertical excitation energies were calculated with the respective unrestricted functional ($T_1$ states) or by TD-DFT calculations ($S_1$ states). The calculations were performed on the bare dianionic species (Fig. 3a).[37]

We took the known photoisomerization pathway of carbonaceous triptycene $6^C$ and the di-$\pi$-borate rearrangement of the tetraarylborate $K[11]$ as blueprints for our mechanistic studies (Fig. 3b and c).[10,11,38] The first reaction step $[6]^{2-} \rightarrow [Int1]^{2-}$ involves C–C coupling between two aryl rings with simultaneous extrusion of one BH unit. In line with experiment, the associated energy barrier of 62.0 kcal $mol^{-1}$ is prohibitively high for a reaction under ambient conditions (in the $S_0$ states). To account for the actually applied photochemical protocol, this crucial step was investigated in detail also for the excited $T_1$ and $S_1$ states of the molecules involved.

First, we verified the basic premise, namely that the Hg lamp employed (emission range: 200–600 nm) does indeed provide the wavelength required to overcome the computed $S_0 \rightarrow S_1$ energy gap of $[6]^{2-}$ ($\Delta E_{S_0 \rightarrow S_1} = 5.068$ eV, corresponding to $\lambda_{exc} = 244.7$ nm; $f_{osc} = 0.1010$).

We scanned the $T_1$ and $S_1$ energy surface topographies along the reaction coordinate between $[6]^{2-}$ and $[Int1]^{2-}$ based on ground-state structures obtained from the $[TS1]^{2-}$-IRC scan (Fig. 4; IRC = intrinsic reaction coordinate): the energy curves for both excited states have minima located downstream of the $[TS1]^{2-}$ structure along the reaction coordinate. It is reasonable that – regardless of a potential intersystem crossing – both these minima may provide access back to the ground state.[39] From that on, a barrierless relaxation leads to $[Int1]^{2-}$ at 36.9 kcal $mol^{-1}$ relative to $[6]^{2-}$. We note that boratanorcaradiene substructures, such as the one present in the key intermediate $[Int1]^{2-}$, have been characterized by XRD in the form of $K[12]$ and $Na[14]$ (Fig. 3c and d).[38,40]

All barriers of the following "walk reaction" on the $S_0$ surface are reachable at ambient conditions:[41] $[Int1]^{2-}$ undergoes a [1,5] sigmatropic shift of the boryl group to form $[Int2]^{2-}$, which is 2.7 kcal $mol^{-1}$ more stable than $[Int1]^{2-}$. The corresponding barrier $[Int1]^{2-} \rightarrow [TS2]^{2-}$ amounts to $\Delta G^{\ddagger} = 17.6$ kcal $mol^{-1}$. A second, slightly endergonic [1,5]sigmatropic shift *via* $[TS3]^{2-}$ gives $[Int3]^{2-}$ ($\Delta G^{\ddagger} = 19.7$ kcal $mol^{-1}$, $\Delta G = 7.9$ kcal $mol^{-1}$). In the last step, C–H activation from $[Int3]^{2-}$ leads to $[10]^{2-}$.[42] The corresponding $[TS4]^{2-}$ lies 12.7 kcal $mol^{-1}$ above $[Int3]^{2-}$, so that the free-energy span to be covered from $[Int2]^{2-}$ to $[TS4]^{2-}$



**Scheme 3** Photoisomerization of $K_2[6]$ to the 8,12b-dihydro-8,12b-diborabenzo[a]fluoranthene derivative $K_2[10]$. (i) Medium-pressure Hg lamp, THF, room temperature, 1 h, quant. conv. by NMR.
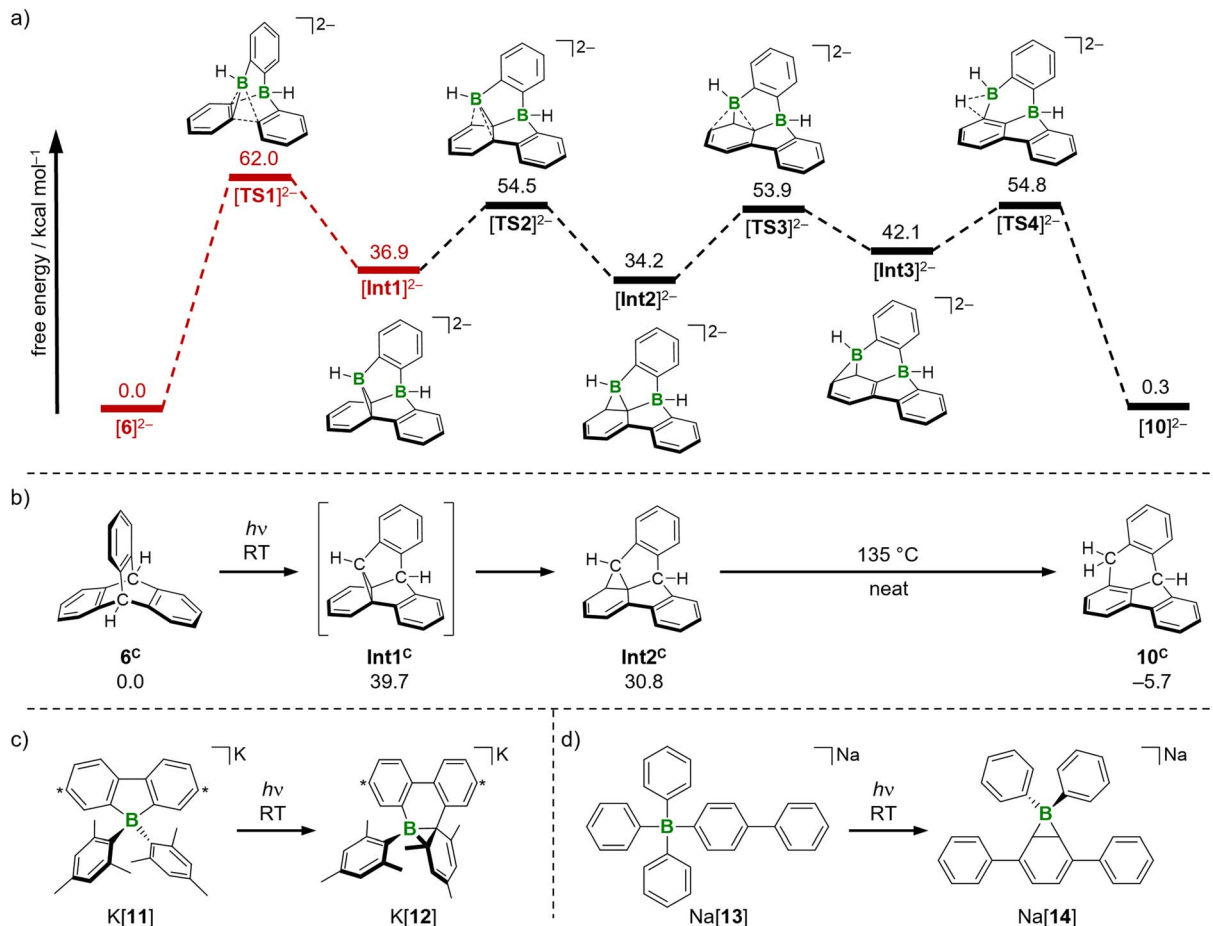
**Fig. 3** (a) Computed mechanism of the photoisomerization $[6]^{2-} \rightarrow [10]^{2-}$ and free energies of intermediates and transition states in their $S_0$ states. The energetically unfavorable and thus photochemically conducted step $[6]^{2-} \rightarrow [Int1]^{2-}$ is marked in red. (b) Literature-reported intermediates of the photoisomerization of triptycene $6^C$ and their calculated free energies (this work). (c) and (d) Known boratanorcaradienes K[**12**] and Na[**14**] obtained from photoreactions of tetraarylborates K[**11**] and Na[**13**], respectively. Carbon atoms marked with asterisks bear t-Bu substituents.
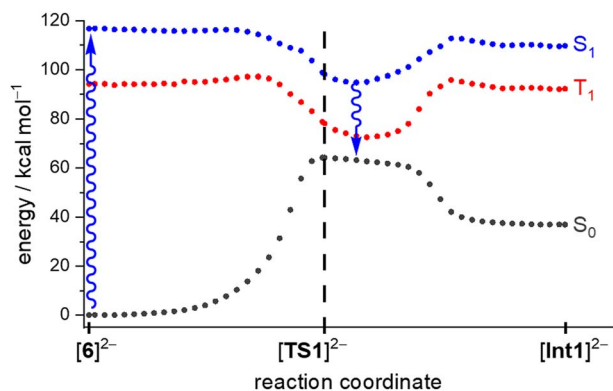


**Fig. 4** Computed energy profiles of the photoinduced reaction $[6]^{2-} \rightarrow [Int1]^{2-}$ in the $S_0$ (gray), $T_1$ (red), and $S_1$ (blue) states. The dashed black line marks the position of $[TS1]^{2-}$ in the ground state; the blue arrows mark the electronic excitation and relaxation (the overall conclusion would remain the same if the relaxation occurred after a putative intersystem crossing from $T_1$).

is 20.6 kcal mol$^{-1}$.[43] The final product $[10]^{2-}$ is essentially iso-energetic to the starting material $[6]^{2-}$. Nevertheless, we consider a reverse reaction unlikely for the following reasons: (i) the energy barrier for the step $[Int1]^{2-} \rightarrow [TS1]^{2-}$ in the reverse reaction is significantly higher (25.1 kcal mol$^{-1}$; Fig. 3) than any barrier downstream $[Int1]^{2-}$ for the forward reaction. (ii) Assuming that the barrier $[Int1]^{2-} \rightarrow [TS1]^{2-}$ could be overcome photochemically, the system would again be in the state described in Fig. 4 and should therefore preferentially fall back to $[Int1]^{2-}$.

## Conclusions

We achieved the synthesis of the parent dianionic 9,10-diboratatriptycene $[6]^{2-}$ and its bridgehead derivatization. In the salt [K(dme)][K(dme)$_2$][**6**], $[6]^{2-}$ acts as a chelating ligand toward both K$^+$ ions, suggesting a possible future use as a tris-benzene ligand for mono- to trinuclear transition metal complexes.[3] Abstraction of a bridgehead H$^-$ substituent releases the free Lewis acid, which is sufficiently long-lived to be trapped by SMe$_2$; this transformation can be carried out at both

bridgehead positions and eventually leads to the neutral boratriptycene-diadduct **9**. By using ditopic Lewis bases, this derivatization chemistry should provide an entry point to polymeric dibora(ta)triptycenes for materials science. The facile photoisomerization of K$_2$[**6**] furnishes the diborabenzo[*a*]-fluoranthene derivative K$_2$[**10**], which combines the two prominent structural motifs of 9,10-dihydro-9,10-diboraanthracene and 9*H*-9-borafluorene and belongs to a virtually unexplored class of B-doped polycyclic aromatic hydrocarbons.

## Data availability

The datasets supporting this article have been uploaded as part of the ESI.†

## Author contributions

S. E. P. performed the experimental studies and characterized all new compounds. S. E. P. and J. G. performed the quantum-chemical calculations. S. V. T., L. C., and M. We. assisted with the synthesis of compounds **9**, [*n*-Bu$_4$N]$_2$[**8**], and Li$_2$[**5**], respectively. M. B. performed the X-ray crystal structure analyses of the compounds [K$_2$(dme)$_3$][**3**], [Li(thf)$_2$][**4**], [K(dme)]-[K(dme)$_2$][**6**], and [K(dme)][K(dme)$_2$][**7**]. A. V. performed the X-ray crystal structure analysis of **9**·CH$_2$Cl$_2$. H.-W. L., F. F., and M. Wa. supervised the project. The manuscript was written by S. E. P., J. G., and M. Wa. and edited by all co-authors.

## Conflicts of interest

There are no conflicts to declare.

## Acknowledgements

## Notes and references

1 C.-F. Chen and Y.-X. Ma, *Iptycenes Chemistry*, Springer Verlag, Berlin, Heidelberg, 2013.

2 M. Woźny, A. Mames and T. Ratajczyk, *Molecules*, 2022, **27**, 250.

3 (*a*) R. A. Gancarz, J. F. Blount and K. Mislow, *Organometallics*, 1985, **4**, 2028–2032; (*b*) P. J. Fagan, M. D. Ward and J. C. Calabrese, *J. Am. Chem. Soc.*, 1989, **111**, 1698–1719; (*c*) H. Schmidbaur, T. Probst and O. Steigelmann, *Organometallics*, 1991, **10**, 3176–3179; (*d*) S. Toyota, H. Okuhara and M. Ōki, *Organometallics*, 1997, **16**, 4012–4015; (*e*) M. Wen, M. Munakata, Y.-Z. Li, Y. Suenaga, T. Kuroda-Sowa, M. Maekawa and M. Anahata, *Polyhedron*, 2007, **26**, 2455–2460.

4 L. Bini, C. Müller, J. Wilting, L. von Chrzanowski, A. L. Spek and D. Vogt, *J. Am. Chem. Soc.*, 2007, **129**, 12622–12623.

5 T. R. Kelly, H. De Silva and R. A. Silva, *Nature*, 1999, **401**, 150–152.

6 T. M. Swager, *Acc. Chem. Res.*, 2008, **41**, 1181–1189.

7 J.-S. Yang and T. M. Swager, *J. Am. Chem. Soc.*, 1998, **120**, 11864–11873.

8 F. Araoka, K.-C. Shin, Y. Takanishi, K. Ishikawa, H. Takezoe, Z. Zhu and T. M. Swager, *J. Appl. Phys.*, 2003, **94**, 279–283.

9 R. Bera, M. Ansari, A. Alam and N. Das, *ACS Appl. Polym. Mater.*, 2019, **1**, 959–968.

10 T. D. Walsh, *J. Am. Chem. Soc.*, 1969, **91**, 515–516.

11 N. J. Turro, M. Tobin, L. Friedman and J. B. Hamilton, *J. Am. Chem. Soc.*, 1969, **91**, 516.

12 A. Lorbach, M. Bolte, H.-W. Lerner and M. Wagner, *Chem. Commun.*, 2010, **46**, 3592–3594.

13 Ö. Seven, S. Popp, M. Bolte, H.-W. Lerner and M. Wagner, *Dalton Trans.*, 2014, **43**, 8241–8253.

14 Wegner *et al.* have postulated such (BN)$_2$-triptycenes as key intermediates of DBA-catalyzed inverse electron-demand Diels–Alder (IEDDA) reactions on higher 1,2-diazenes: (*a*) S. N. Kessler and H. A. Wegner, *Org. Lett.*, 2010, **12**, 4062–4065; (*b*) S. N. Kessler, M. Neuburger and H. A. Wegner, *J. Am. Chem. Soc.*, 2012, **134**, 17885–17888; (*c*) L. Schweighauser, I. Bodoky, S. N. Kessler, D. Häussinger, C. Donsbach and H. A. Wegner, *Org. Lett.*, 2016, **18**, 1330–1333; (*d*) L. Schweighauser and H. A. Wegner, *Chem.–Eur. J.*, 2016, **22**, 14094–14103; (*e*) L. Hong, S. Ahles, M. A. Strauss, C. Logemann and H. A. Wegner, *Org. Chem. Front.*, 2017, **4**, 871–875; (*f*) S. Ahles, S. Götz, L. Schweighauser, M. Brodsky, S. N. Kessler, A. H. Heindl and H. A. Wegner, *Org. Lett.*, 2018, **20**, 7034–7038; (*g*) S. Ahles, J. Ruhl, M. A. Strauss and H. A. Wegner, *Org. Lett.*, 2019, **21**, 3927–3930.

15 (*a*) F. Jäkle, T. Priermeier and M. Wagner, *J. Chem. Soc., Chem. Commun.*, 1995, 1765–1766; (*b*) E. Herdtweck, F. Jäkle, G. Opromolla, M. Spiegler, M. Wagner and P. Zanello, *Organometallics*, 1996, **15**, 5524–5535; (*c*) F. Jäkle, T. Priermeier and M. Wagner, *Organometallics*, 1996, **15**, 2033–2040; (*d*) E. Herdtweck, F. Jäkle and M. Wagner, *Organometallics*, 1997, **16**, 4737–4745.

16 M. Henkelmann, A. Omlor, M. Bolte, V. Schünemann, H.-W. Lerner, J. Noga, P. Hrobárik and M. Wagner, *Chem. Sci.*, 2022, **13**, 1608–1617.

17 A. Ben Saida, A. Chardon, A. Osi, N. Tumanov, J. Wouters, A. I. Adjieufack, B. Champagne and G. Berionni, *Angew. Chem., Int. Ed.*, 2019, **58**, 16889–16893.

18 A. Chardon, A. Osi, D. Mahaut, T.-H. Doan, N. Tumanov, J. Wouters, L. Fusaro, B. Champagne and G. Berionni, *Angew. Chem., Int. Ed.*, 2020, **59**, 12402–12406.

19 A. Osi, D. Mahaut, N. Tumanov, L. Fusaro, J. Wouters, B. Champagne, A. Chardon and G. Berionni, *Angew. Chem., Int. Ed.*, 2022, **61**, e202112342.

20 A. Osi, N. Tumanov, J. Wouters, A. Chardon and G. Berionni, *Synthesis*, 2023, **55**, 347–353.

21 (*a*) A. Hübner, A. M. Diehl, M. Diefenbach, B. Endeward, M. Bolte, H.-W. Lerner, M. C. Holthausen and M. Wagner, *Angew. Chem., Int. Ed.*, 2014, **53**, 4832–4835; (*b*) A. Hübner, T. Kaese, M. Diefenbach, B. Endeward, M. Bolte,

H.-W. Lerner, M. C. Holthausen and M. Wagner, *J. Am. Chem. Soc.*, 2015, **137**, 3705–3714.

22 Very recently, Marder *et al.* disclosed that thermal rearrangement of 1,2-bis-(9-borafluorenyl)benzene leads to a diborabenzo[*a*]fluoranthene derivative: J. Krebs, A. Häfner, S. Fuchs, X. Guo, F. Rauch, A. Eichhorn, I. Krummenacher, A. Friedrich, L. Ji, M. Finze, Z. Lin, H. Braunschweig and T. B. Marder, *Chem. Sci.*, 2022, **13**, 14165–14178.

23 (*a*) G. Wittig and F. Bickelhaupt, *Chem. Ber.*, 1958, **91**, 883–894; (*b*) H. J. S. Winkler and G. Wittig, *J. Org. Chem.*, 1963, **28**, 1733–1740; (*c*) M. A. G. M. Tinga, O. S. Akkerman, F. Bickelhaupt, E. Horn and A. L. Spek, *J. Am. Chem. Soc.*, 1991, **113**, 3604–3605.

24 See the ESI† for more details.

25 (*a*) E. von Grotthuss, S. E. Prey, M. Bolte, H.-W. Lerner and M. Wagner, *Angew. Chem., Int. Ed.*, 2018, **57**, 16491–16495; (*b*) E. von Grotthuss, S. E. Prey, M. Bolte, H.-W. Lerner and M. Wagner, *J. Am. Chem. Soc.*, 2019, **141**, 6082–6091; (*c*) S. E. Prey and M. Wagner, *Adv. Synth. Catal.*, 2021, **363**, 2290–2309; (*d*) S. E. Prey, C. Herok, F. Fantuzzi, M. Bolte, H.-W. Lerner, B. Engels and M. Wagner, *Chem. Sci.*, 2023, **14**, 849–860.

26 A. Lorbach, M. Bolte, H.-W. Lerner and M. Wagner, *Organometallics*, 2010, **29**, 5762–5765.

27 E. von Grotthuss, F. Nawa, M. Bolte, H.-W. Lerner and M. Wagner, *Tetrahedron*, 2019, **75**, 26–30.

28 H. Nöth and B. Wrackmeyer, Nuclear magnetic resonance spectroscopy of boron compounds, in *NMR Basic Principles and Progress*, ed. P. Diehl, E. Fluck and R. Kosfeld, Springer Verlag, Berlin, Heidelberg, New York, 1978.

29 We performed the cycloaddition reaction of M$_2$[**2**] with M$^+$ = Li$^+$, Na$^+$, and K$^+$. Since crystallization is the key purification step and K$_2$[**6**] gave the most reproducible yields, we focused on this compound throughout this work.

30 Values refer to [K(Me$_6$-tren)][HBPh$_3$] (Me$_6$-TREN = *N,N,N*-tris(2-(dimethylamino)ethyl)amine): D. Mukherjee, H. Osseili, T. P. Spaniol and J. Okuda, *J. Am. Chem. Soc.*, 2016, **138**, 10790–10793.

31 The reaction was monitored by $^1$H NMR spectroscopy in CD$_2$Cl$_2$, and the resonances of the byproducts CD$_2$HCl and CD$_2$H$_2$ were detected as characteristic 1:2:3:2:1 quintets. Comparable chlorination of a siladodecahedrane in CD$_2$Cl$_2$ was recently reported: M. Bamberg, M. Bursch, A. Hansen, M. Brandl, G. Sentis, L. Kunze, M. Bolte, H.-W. Lerner, S. Grimme and M. Wagner, *J. Am. Chem. Soc.*, 2021, **143**, 10865–10871.

32 S. J. Lancaster and D. L. Hughes, *Dalton Trans.*, 2003, 1779–1789.

33 J.-M. Denis, H. Forintos, H. Szelke, L. Toupet, T.-N. Pham, P.-J. Madec and A.-C. Gaumont, *Chem. Commun.*, 2003, 54–55.

34 To compare the photochemical responses of K$_2$[**6**] and its all-carbon congener **6**$^C$, both molecules were irradiated under identical conditions (see the ESI†). We observed a significantly faster reaction in the case of K$_2$[**6**] and have shown that the reactions lead to different scaffolds: while irradiation of K$_2$[**6**] cleanly furnishes K$_2$[**10**], the reaction of **6**$^C$ stops at the stage of **Int2**$^C$. The isomerization to **10**$^C$ requires heating, *cf.* ref. 10 and 11.

35 A. V. Marenich, C. J. Cramer and D. G. Truhlar, *J. Phys. Chem. B*, 2009, **113**, 6378–6396.

36 J.-D. Chai and M. Head-Gordon, *Phys. Chem. Chem. Phys.*, 2008, **10**, 6615–6620.

37 The exclusion of the counter cations is justified by two facts: (*i*) Unlike Li$^+$ ions, K$^+$ ions do not form strong contact ion pairs in solution that influence the reactivity of the compounds, see ref. 25b; (*ii*) Omitting K$^+$ ions and their coordinating thf ligands in the calculations reduces the computational cost significantly, see ref. 25d.

38 J. Radtke, S. K. Mellerup, M. Bolte, H.-W. Lerner, S. Wang and M. Wagner, *Org. Lett.*, 2018, **20**, 3966–3970.

39 S. Wang, K. Yuan, M.-F. Hu, X. Wang, T. Peng, N. Wang and Q.-S. Li, *Angew. Chem., Int. Ed.*, 2018, **57**, 1073–1077.

40 J. D. Wilkey and G. B. Schuster, *J. Am. Chem. Soc.*, 1991, **113**, 2149–2155.

41 A comparable [1,5]sigmatropic shift, also known as "walk reaction", has been studied for norcaradiene: (*a*) F.-G. Klärner, *Angew. Chem., Int. Ed.*, 1974, **13**, 268–270; (*b*) A. Kless, M. Nendel, S. Wilsey and K. N. Houk, *J. Am. Chem. Soc.*, 1999, **121**, 4524–4525.

42 The [**TS4**]$^{2-}$-IRC scan indicates a bifurcation at the C–H activation step because the energy profile shows a plateau between [**Int3**]$^{2-}$ and [**TS4**]$^{2-}$ (see Fig. S55†). At the end of this plateau, the molecular geometry is sufficiently close to that of [**TS3**]$^{2-}$ for [**TS3**]$^{2-}$ to be optimized without significant energy and geometry changes. Consequently, a shortcut [**Int2**]$^{2-}$ → [**TS3**]$^{2-}$ → [**TS4**]$^{2-}$ → [**10**]$^{2-}$ is also likely to occur: D. H. Ess, S. E. Wheeler, R. G. Iafe, L. Xu, N. Çelebi-Ölçüm and K. N. Houk, *Angew. Chem., Int. Ed.*, 2008, **47**, 7592–7601.

43 We also located a transition state directly connecting [**Int2**]$^{2-}$ and [**10**]$^{2-}$ ([**TS4′**]$^{2-}$, $\Delta G^{\ddagger}$ = 40.3 kcal mol$^{-1}$, see Fig. S54†). However, since the energy required for the latter is significantly higher than for the above-mentioned path *via* [**TS4**]$^{2-}$, the contribution of [**TS4′**]$^{2-}$ should be negligible.